Revision 2 (September 10, 2012)

Eclogitic clasts with omphacite and pyrope-rich garnet in the NWA 801 CR2 chondrite

Makoto Kimura[1,*], Naoji Sugiura[2], Takashi Mikouchi[2], Takao Hirajima[3], Hajime Hiyagon[2], and Yoshie Takehana[2]

[1]Faculty of Science, Ibaraki University, Bunkyo 2-1-1, Mito 310-8512, Japan

[2]Department of Earth and Planetary Science, Graduate School of Science, University of Tokyo, Hongo, Bunkyo-Ku, Tokyo 113-0033, Japan

[3]Department of Geology and Mineralogy, Graduate School of Science, Kyoto University, Kitashirakawa Oiwakecho, Sakhyo-ku, Kyoto 606-8502, Japan

*E-mail: makotoki@mx.ibaraki.ac.jp

Submitted for publication in American Mineralogist

ABSTRACT

We report mineral assemblages from three clasts in the Northwest Africa 801 CR chondrite. The clasts, 1-3 mm in size, are ellipsoidal to irregular-shaped, and show similar granular texture. The constituent minerals in the clasts are omphacite and pyrope-rich garnet, in addition to olivine and orthopyroxene. The omphacite contains jadeite (34mole%) and diopside-hedenbergite (37%), and a significant amount of an enstatite-ferrosilite component (19%), which distinguishes it from terrestrial omphacite. The omphacite has a disordered C2/c structure. Graphite, phlogopite, chlorapatite, Fe-Ni metal, troilite and pentlandite are present as minor minerals in the clasts. The minerals commonly found in chondrites, such as plagioclase and spinel group minerals, are not found in these clasts. Aluminum and sodium in the clasts are completely partitioned into omphacite and garnet. The mineral assemblages and compositions of the clasts are similar to those in terrestrial eclogite, except for the occurrence of olivine and some mineral chemistry, and this is the first discovery of an extraterrestrial eclogitic mineral assemblage. The clasts formed under high-pressure conditions, 2.8-4.2GPa and 940-1080°C, as estimated from a set of conventional geothermobarometers, indicative of formation in a large parent body. Another possibility is impact-induced origin, although the formation conditions would have been different from those for known shock veins. Meteorites usually consist of minerals that formed under low-pressure conditions, except for ultrahigh-pressure minerals found in shock veins. However, this study suggests that the pressure conditions for meteorite formation vary much wider than previously understood.

Keywords: CR chondrite, clast, omphacite, pyrope, eclogite

INTRODUCTION

The most common silicate minerals in chondrites are olivine, Ca-poor and -rich pyroxenes, and plagioclase, which formed under low-pressure conditions, less than 0.1GPa (Heyse 1978). Less common are ultrahigh-pressure minerals, such as ringwoodite and majorite, present in impact-induced shock melt veins and which formed at pressures of ~20GPa, during impact processes on the parent bodies (e.g., Chen et al. 1996; Ohtani et al. 2004). Plagioclase can be transformed to maskelynite during impact processes. Also rare in chondrites is the occurrence of hornblende, recently found in an R chondrite, which formed at pressures of $<\sim$0.1GPa during impact (McCanta et al. 2008; Ota et al. 2009).

Thus, the mineralogy of chondrites, except some phases formed during impact processes, is consistent with their origin in small (asteroid-size) parent bodies. This is supported by the calculated radii of parent asteroids for most chondrites to be smaller than ~100 km (e.g., Miyamoto et al. 1981). The absence of high-pressure (H*P*) mineral assemblages in chondrites, typical of those in terrestrial regional metamorphic rocks, also supports an origin in small asteroids. However, here we report the first discovery of a H*P* mineral assemblage, containing both omphacite and pyrope-rich garnet, in clasts in a CR chondrite.

CR chondrites are among the most primitive chondrites. They are characterized by distinguishing features, such as the occurrence of Fe-Ni metal with solar Ni:Co ratios. CR and related CH and CB chondrites have unique nitrogen isotopic compositions (Weisberg et al. 1993). Besides their common constituents, such as chondrules, Fe-Ni metal, and matrix, some CR chondrites have unusual clasts containing kaersutite and graphite (Abreu and Brearley 2007; Sugiura et al. 2008). Such clasts are expected to help constrain the complicated formation process of the primitive chondrites.

In this paper we present our results on the mineralogy of three clasts in the North West Africa (hereafter NWA) 801 CR chondrite, and discuss a H*P* origin for them. Sugiura et al. (2008) and Kimura et al. (2010) preliminarily reported some unusual features of these clasts.

SAMPLES AND EXPERIMENTAL METHODS

We investigated three polished thin sections cut from the same chip of the NWA 801 chondrite. Each section contains an unusual clast (#2, 3 and 6), respectively, although they are probably different portions of the same clast.

Quantitative mineral analyses were conducted using an electron-probe microanalyzer, and the crystalline nature of the constituent minerals was determined using an electron back-scatter diffraction (EBSD) system. These analytical methods were the same as those reported by Kimura et al. (2009). We also identified minerals using the JASCO NRS-1000 laser Raman microspectrometer at the National Institute of Polar Research, with a wavelength of 531.91 nm and an intensity of 11 mW of laser beam.

PETROGRAPHY AND MINERALOGY

The three clasts, 1-3 mm in size, are ellipsoidal to irregular in shape. They are embedded among chondrules and matrix and have sharp boundaries with the matrix (Fig. 1a). The constituent minerals are usually 5-40μm in size (Fig. 1b), and all the clasts show a similar granular texture, except for ~10 vol.% of fine-grained areas (less than a few μm in grain size) in clast #3. Chondrule relics and a remarkable large grain size have been described in a CR clast by Abreu and Brearley (2007). These types of clasts were not found in our study.

The clasts we found mainly consist of silicate minerals, minor Fe-Ni metal and sulfides with terrestrial weathering products of the latter, mainly Fe oxide (Table 1). The major minerals, identified by electron microprobe analyzer, are olivine, two kinds of pyroxene, Ca-poor and Na-Al-rich, and garnet. Olivine and Ca-poor pyroxene show euhedral to subhedral forms. Olivine is the dominant mineral, making up ~70vol.% of the silicate minerals in the clasts.

A distinct feature of the clasts is the absence of the common minor minerals that are typically found in chondrites, such as diopside, plagioclase and spinel group minerals. Feldspathic glass and maskelynite do not occur in the clasts. Instead, Na-Al-rich pyroxene (omphacite) and garnet, minerals that are extremely rare in meteorites, are common in these clasts. They occur as anhedral to subhedral grains, 5-20μm in size (Fig. 1b).

Another characteristic feature is the minor occurrence of lath-shaped graphite, as described previously in a CR clast (Abreu and Brearley 2007) and in graphite-bearing xenoliths in an LL3 chondrite (Semenenko et al. 2004). Graphite abundance and distribution varies among the clasts; clast #3 does not contain graphite, whereas graphite in clast #6 is about ~1vol.%. Clast #2 has two lithologies (Table 1), graphite-bearing (~10 vol. % of this clast) and graphite-free. In clast #2, graphite is present along silicate grain boundaries and within olivine and Ca-poor pyroxene. A small amount of phlogopite is encountered in graphite-free lithology of #2, whereas the other clasts are almost free of this mineral. Other minor minerals, Ca-phosphate, Fe-Ni metal, troilite, and pentlandite are present in all three clasts, although they are heavily (terrestrially) weathered.

Table 2 shows representative compositions of minerals in the clasts. Olivine (Fo_{66-68}, $Fo_{67.2}$ on average) is nearly homogeneous in composition in all of the clasts (Table 1). The MnO and CaO contents are 0.2-0.4 and <0.2wt. %, respectively, and the Cr_2O_3 and NiO contents are below detection limits (0.1%). Ca-poor pyroxene shows compositional variation (Fig. 2). However, most of the pyroxene is nearly homogeneous (ranging from $En_{70-75}Wo_{0.3-1.1}$, $En_{73.2}Fs_{26.1}Wo_{0.7}$ on average), and only a few coarse grains, 50-80 μm in size, in the clasts #2 and #6 contain Mg-rich cores ($En_{78-87}Wo_{0.4-3}$) (Fig. 1c). Ca-poor pyroxene, excluding the Mg-rich core, contains <0.1wt.% TiO_2, 0.3-1.4 Al_2O_3, 0.1-1.0 Cr_2O_3, and <0.3 Na_2O. The minor element concentrations in the Mg-rich core are almost the same (<0.1wt.% TiO_2, 0.2-1.4 Al_2O_3, 0.3-1.1 Cr_2O_3, and <0.3 Na_2O) as the homogeneous Mg-poor pyroxenes. The graphite-free lithology in clast #2 does not contain Ca-poor pyroxene.

Na-Al-rich pyroxenes from the three clasts are similar in composition, and contain 6.9-9.3wt.% (7.9wt.% on average) Al_2O_3, 2.1-4.1 (3.4) Cr_2O_3, 5.0-7.9 (6.4) FeO, 9.6-11.5 (10.5) MgO, 8.5-11.5 (9.7) CaO, and 5.5-6.9 (6.2) Na_2O. It also contains 0.2-0.8wt.% TiO_2 and <0.3 MnO. The NiO and K_2O contents are below detection limits (0.1 and 0.04%, respectively). The average chemical formula is $(Na_{0.44}Ca_{0.37}Mg_{0.57}Fe_{0.19}Cr_{0.10}Al_{0.32})_{1.99}(Al_{0.01}Si_{1.99})_{2.00}O_6$. This stoichiometric chemical composition suggests that the Na-Al-rich pyroxene is omphacitic pyroxene without aegirine and esseneite components. It also contains a significant amount of a Na-pyroxene component (jadeite 34mole% and kosmochlor 10% on average) and a diopside-hedenbergite (37%) component (Fig. 3). Furthermore, it contains an enstatite-ferrosilite component (19%). This is a unique characteristic that distinguishes it from terrestrial omphacite, which mostly consists of jadeite and diopside-hedenbergite, with a minor aegirine component (e.g., Deer et al. 1992).

Garnet is nearly homogeneous in all the clasts (Fig. 4), and contains 20.0-21.2 wt. % (20.7 wt. % on average) Al_2O_3, 1.7-3.4 (2.4) Cr_2O_3, 19.0-21.6 (20.0) FeO, 10.8-13.3 (12.6) MgO, and 2.1-4.4 (3.1) CaO. The garnet also contains <0.2 wt. % TiO_2, 0.7-1.2 MnO, and <0.2 Na_2O. The average chemical formula is $(Mg_{1.40}Fe_{1.27}Ca_{0.26}Mn_{0.06})_{2.99}(Al_{1.85}Cr_{0.14})_{1.99}Si_{3.01}O_{12}$, suggesting there is no andradite component. The chemical composition is indicative of pyrope-rich garnet with a large amount of almandine and minor grossular components.

Since these phases have many polymorphs, we identified them using the laser Raman micro-spectrometer. The constituent minerals were identified as olivine (main bands at 855 and 823cm^{-1}), garnet (919, 852, 682, 556, and 354cm^{-1}), orthopyroxene (for Ca-poor pyroxene) (1007, 680, 662, 398, and 337cm^{-1}), and disordered graphite (1588 and 1357cm^{-1}). These results were supported by EBSD data. Ultra-H*P* polymorphs, such as ringwoodite, majorite, and diamond, were not identified in the clasts.

Omphacite has two kinds of polymorphic structure; C2/c is a higher-temperature (>800°C) disordered phase and P2/n is a lower-temperature ordered phase (Carpenter 1980). We determined the crystalline nature of omphacite (Na-Al-rich pyroxene) in the clasts by EBSD. The patterns obtained match those of omphacite which does not have a P2/n type structure, but is C2/c (McCormick et al. 1989) (Fig. 5). Based on the Raman data, two crystal structures can be distinguished (Katerinopoulou et al. 2008). The observed main bands, 1015, 680, 399, and 343cm^{-1}, support the identification for C2/c. From the crystalline nature, the omphacite studied here could be a high-temperature polymorph. However, a significant amount of enstatite-ferrosilite component may affect the phase boundary between the ordered/disordered phases for the omphacite as the aegirine component does in terrestrial omphacite (Carpenter 1980; Matsumoto and Hirajima 2005).

Ca-phosphate is chlorapatite (Table 2). Fluorine was not detected with the electron-probe microanalyzer. Phlogopite contains 3.3wt.% TiO_2 (on average), 11.7 FeO, 17.1 MgO, 1.1 Na_2O and 7.2 K_2O. Fe-Ni metal and pentlandite contain 8.2-24.6wt.% and 19.1-25.3 Ni, and 0.5-1.1 and 1.6-1.7 Co, respectively.

We calculated the temperature and pressure conditions by the set of conventional geothermobarometers using coexisting olivine, pyroxenes, and garnet in the clasts. We applied the following geothermobarometers to the clasts: orthopyroxene-clinopyroxene (Taylor 1998), garnet-clinopyroxene (Nimis and Taylor 2000; Krogh Ravna 2000), garnet-orthopyroxene (Harley 1984; Nickel and Green 1985; Brey and Köhler 1990), and garnet-olivine (O'Neil and Wood 1979). Figure 6 shows representative results for the mineral assemblage in the clast #6. Estimated pressure is 2.8-4.2GPa and 940-1080°C for this clast. Most of these geothermobarometers have been developed to estimate the physical conditions for the terrestrial rocks, and mineral chemistries in the clasts are not always similar to those in terrestrial rocks as mentioned before. Nevertheless, the results of these geothermobarometers are consistent with one another. Therefore, the results should reflect the physical condition of the clast although including some errors from such differences in mineral chemistry.

We calculated oxygen fugacity for the clast from the conditions mentioned above. The calculation method and the reaction, $Fe + FeSiO_3 + 1/2\ O_2 = Fe_2SiO_4$, are the same as those used by Righter and Drake (1996). The oxygen fugacity for the clast is 1.0 log fO_2 lower than the IW buffer, which is close to those for ordinary chondrite, 1.2-1.5 log fO_2 lower than the IW (Righter and Drake, 1996).

DISCUSSION

The characteristic features of the 3 clasts in NWA 801 are clearly different from those of the host CR chondrite; the clasts show highly equilibrated textures, and do not contain chondrules, matrix, or any evidence of once having chondrules (e.g., chondrule relics). The texture of the clasts is in part similar to those of highly equilibrated chondrites, and a graphite-bearing clast previously described in a CR chondrite (Abreu and Brearley 2007; Semenenko et al. 2004). However, the mineral assemblages of the clasts, including both omphacite and pyrope-rich garnet, are distinct from those in any known meteorites. The absence of plagioclase and spinel group minerals is a characteristic in the NWA 801 clasts. However, the clasts are not Al-free; all of the

Al is partitioned into the omphacite and garnet.

Sub-micrometer-size omphacite, <300nm, has been reported from the Zagami martian meteorite (Langenhorst and Poirier 2000). It occurs with stishovite and $KAlSi_3O_8$ with hollandite structure in shock veins that formed under pressures <25GPa. Pyrope-rich garnet, sub-micrometer in size, was discovered in Novo Urei (ureilite) (Mitreikina et al. 1994) and micrometer-size pyrope-rich garnet was found in Gujba (CB chondrite) (Weisberg and Kimura 2010). The garnet in Gujba is present near majorite and wadsleyite-bearing shock veins that formed at pressures of ~19GPa. On the other hand, omphacite and garnet in the NWA 801 clasts are much larger, 5-20μm in size, and always coexist with olivine and orthopyroxene. The estimated pressure for this assemblage is much lower than those for Gujba and Zagami. Thus, the occurrences, mineral assemblages, and formation conditions of omphacite and pryope-rich garnet previously reported in meteorites, are clearly different from those in the NWA 801 clasts. Our discovery is the first reported occurrence of an extraterrestrial eclogitic H*P* mineral assemblage represented by both omphacite and pyrope-rich garnet.

The observed mineral assemblage of the clasts, garnet + omphacite + orthopyroxene + olivine ± phlogopite, is essentially similar to those in eclogite facies rocks of ultramafic and mafic compositions, but with some exceptions. In terrestrial eclogites with mafic compositions (such as in the Western Gneiss region, Norway), orthopyroxene-bearing eclogitic assemblages are rare, but olivine-bearing ones are not (e.g., Carswell 1990). Although a 5 phases assemblage is commonly observed in garnet peridotites on the Earth, clinopyroxene compositions in the terrestrial garnet peridotites are characterized by lower-Na_2O contents (<1.0wt.%; Carswell 1990) and the average olivine is around Fo_{90} (e.g., Naemura et al. 2009). Furthermore, the high sodic and enstatite-ferrosilite contents in omphacite, the low Al_2O_3 content in orthopyroxene, and the high Fa content in olivine in the NWA 801 clasts, as mentioned before, are reflections of the unique formation conditions and precursor materials in the parental asteroid, compared with those of terrestrial metamorphic rocks.

Although there are some mineralogical differences between the clasts and terrestrial eclogites, calculated pressure-temperature conditions for the clasts are in the stability field of high-temperature type terrestrial eclogites (Carswell 1990). Such pressure conditions are consistent with the occurrence of graphite, because diamond is stable under relatively higher pressures (Fig. 6). The graphite-CO-CO_2 buffer has been determined experimentally (e.g., LaTourrette and Holloway 1994; Frost and Wood 1997). Under the oxygen fugacity and formation conditions as mentioned above, graphite should be stable in the clasts, consistent with the occurrence. The estimated oxygen fugacity is close to those for ordinary chondrites, but much lower than those for R and CK chondrites (Righter and Drake 1996; Righter and Neff 2007). This is consistent with no apparent ferric iron-bearing phases in the clasts, whereas R and CK chondrites contain magnetite and NiO in olivine.

Lath-shaped graphite, and euhedral olivine and orthopyroxene suggest that these clasts formed by crystallization from a melt. Thus, we expect that olivine and orthopyroxene may have had primary igneous zoning. Since the pressure dependence of the diffusion coefficient in orthopyroxene is not known, we calculated diffusion distances using atmospheric pressure data (Dohmen et al. 2007; Ganguly and Tazzoli 1994). Olivine that is 20μm in size becomes completely homogeneous during several days at 1000°C, whereas the diffusion length in orthopyroxene is less than a few micrometers under the same conditions. Thus, if the parent material of the clasts was preserved in the interior of an asteroid for several days at ~1000°C, we would expect the olivine to become homogeneous, whereas orthopyroxene should partly preserve its primary compositional variation. This could explain the Mg-rich cores of a few of the coarse orthopyroxene grains which are associated with homogeneous olivine (Fig. 1c).

The thermal history and the H*P* condition seem to suggest crystallization of the clasts in the deep interior of a large parent body. Abreu and Brearley (2007) suggested that kaersutite-graphite-bearing clasts in a CR chondrite formed deep in the asteroid's interior, far from the surface. However, the H*P* conditions, ~3GPa, correspond to the center of a parent body with a 1500 km in radius, assuming a chondritic parent body (Hartmann 2005). Although such a large asteroid is not observed in the current solar system, Goldstein et al. (2009) suggested that iron meteorites were originally derived from bodies as large as 1000km or more in size. We cannot totally rule out the existence of a large chondritic parent body in the early solar system, which was later broken.

Another possibility is that the eclogitic clasts formed from impact-induced heating in the interior of a much smaller parent body, similar in size to known asteroids. Impact-induced shock melt veins containing ultra-H*P* minerals were locally formed on meteorite parent bodies under much higher pressures than that for the clasts. Although such veins also contain garnet, it is majorite with minor pyrope component, and usually smaller than several microns in size (Ohtani et al. 2004). Pyrope-rich garnet along with omphacite encountered in the clasts have not been found in shock veins. Therefore, even if the clasts were formed by impact, the formation conditions of the clasts were evidently different from those for known shock veins.

Naemura et al. (2009) noted that geothermobarometers systematically show different results for terrestrial peridotites; those by Taylor (1998) and Krogh Ravna (2000) are lower than those of Harley (1984) and O'Neil and Wood (1979). Naemura et al. (2009) suggested that the latter geothermobarometers may not give equilibrium conditions for the terrestrial peridotites. On the other hand, Fig. 6 shows that the results obtained by the same set of geothermobarometers are consistent with one another. A possible explanation for the difference in results between terrestrial eclogites and the NWA 801 clasts is the higher FeO content and the abundant enstatite-ferrosilite component in omphacite, which is not present in terrestrial omphacites. Alternatively, it is probable that the clasts cooled rapidly from the H*P* conditions, which are consistent with all of the geothermobarometers applied here. This may be consistent with the survival of omphacite with a high-temperature structure and the Mg-rich cores of the orthopyroxene grains in the clasts. The parent asteroid of the clasts might have been disrupted before the interior cooled to low-temperatures, and as a result the clasts cooled rapidly.

It is believed that meteorites formed in small asteroidal bodies under very low-pressure conditions, except for the high pressures produced during secondary impact events, as recorded in features such as shock veins. However, here we report mineral assemblages similar to those of terrestrial metamorphic rocks formed under H*P* conditions in a planet-sized body. The pressure conditions estimated for the NWA 801 clasts are intermediate between those recorded for the primary formation of meteorites and those recorded in secondary shock veins. Our discovery indicates that the range of pressure conditions for meteorite formation was much more variable than previously considered.

The precursor materials of the clasts, and the genetic relationships between the clasts and the host CR chondrite are not yet clear. We are now measuring the isotopic and trace element compositions of the clasts which will shed light on this issue.

ACKNOWLEDGEMENTS

We thank A. Yamaguchi who helped to use laser Raman microspectrometer, and K. Naemura for calculation of some geothermobarometries. We appreciate the critical reading of the manuscript by M. K. Weisberg, and the careful reviews by T. J. Fagan and K. Righter. We also thank the associate editor R. H. Jones for efficient handling of the manuscript. This work was supported by a Grant-in-aids of Ministry of Education, Science, Sport, and Culture of Japanese

government, No. 22540488 to M. K.

REFERENCES

Abreu, N.M. and Brearley, A.J. (2007) A unique graphite and amphibole-bearing clast in QUE 99177: an extensively metamorphosed xenolith in a pristine CR3 chondrite (abstract). Lunar and Planetary Science, XXXVIII, 2419.pdf.

Brey, G. P. and Köhler, T. (1990). Geothermobarometry in Four-phase Lherzolites II. New thermobarometers, and practical assessment of existing thermobarometers. Journal of Petrology **31**, 1353–1378.

Bundy, F.R. (1980) The P,T phase and reaction diagram for elemental carbon. Journal of Geophysical Research, 85, 6930-6938.

Carpenter, M.A. (1980) Mechanisms of exsolution in sodic pyroxene. Contributions to Mineralogy and Petrology, 71, 289-300.

Chen, M., Sharp, T.G., El Goresy, A., Wopenka, B., and Xie, X. (1996) The majorite-pyrope + magnesiowüstite assemblage: Constraints on the history of shock veins in chondrites. Science, 271, 1570-1573.

Carswell, D.A. (1990) Eclogite facies rocks, 396p. Blackie Academic & Professional, London.

Deer, W.A., Howie, R.A., and Zussman, J. (1992) An Introduction to the Rock-Forming Minerals, Second Edition, 696p. Longman, Harlow.

Dohmen, R., Becker, H.-W., and Chakraborty, S. (2007) Fe–Mg diffusion in olivine I: experimental determination between 700 and 1,200 °C as a function of composition, crystal orientation and oxygen fugacity. Physics and Chemistry of Minerals, 34, 389-407.

Frost, D.J. and Wood, BAJA. (1997) Experimental measurements of the fugacity of C02 and graphite/diamond stability from 35 to 77 kbar at 925 to 1650°C. Geochimica et Cosmochimica Acta, 61, 1565-1574.

Ganguly, J. and Tazzoli, V. (1994) Fe^{2+}-Mg interdiffusion in orthopyroxene: Retrieval from the data on intracrystalline exchange reaction. American Mineralogist, 79, 930-937.

Goldstein J. I., Scott E. R. D., and Chabot N. L. (2009) Iron meteorites: Crystallization, thermal history, parent bodies, and origin. Chemie der Erde 69, 293-325.

Harley, S.L. (1984) An experimental study of the partitioning of Fe and Mg between garnet and orthopyroxene. Contributions to Mineralogy and Petrology, 86, 359-373.

Hartmann, W.K. (2005) Moons & Planets, 428p. Brooks/Cole, Belmont.

Heyse, J.V. (1978) The metamorphic history of LL-group ordinary chondrites. Earth and Planetary Science Letters, 40, 365-381.

Katerinopoulou, A., Musso, M., and Amthauer, G. (2008) A Raman spectroscopic study of the phase transition in omphacite. Vibrational Spectroscopy, 48, 163-167.

Kimura, M., Mikouchi, T., Suzuki, A., Miyahara, M., Ohtani, E., and El Goresy, A. (2009) Kushiroite, $CaAlAlSiO_6$: A new mineral of the pyroxene group from the ALH 85085 CH chondrite, and its genetic significance in refractory inclusions. American Mineralogist, 94, 1479-1482.

Kimura, M., Sugiura, N., Hiyagon, H., Mikouchi, T., and Takehana, Y. (2010) Unusual clasts including pyrope-almandine garnet and omphacitic pyroxene in the Northwest Africa 801 CR2 chondrite (abstract). Meteoritics and Planetary Science, 45, A105.

Krogh Ravna, E. (2000) The garnet–clinopyroxene Fe^{2+}–Mg geothermometer: an updated calibration. Journal of Metamorphic Geology, 18, 211-219.

Langenhorst, F. and Poirier, J.P. (2000) 'Eclogitic' minerals in a shocked basaltic meteorite. Earth and Planetary Science Letters, 176, 259-265.

LaTourrette, T. and Holloway, J.R. (1994) Oxygen fugacity of the diamond+C-O fluid assemblage and CO2 fugacity at 8GPa. Earth and Planetary Science Letters, 128, 439-451.

Matsumoto, K. and Hirajima, T. (2005) The coexistence of jadeite and omphacite in an eclogite-facies metaquartz diorite from the southern Sesia Zone, Western Alps, Italy. Journal of Mineralogical and Petrological Sciences, 100, 70-84.

McCanta, M.C., Treiman, A.H., Dyar, M.D., Alexander, C.M.O.D., Rumble, D., III, and Essene, E.J. (2008) The LaPaz Icefield 04840 meteorite: Mineralogy, metamorphism, and origin of an amphibole- and biotite-bearing R chondrite. Geochimica et Cosmochimica Acta, 72, 5757-5780.

McCormick, T.C., Hazen, R.M., and Angel, R.J. (1989) Compressibility of omphacite to 60 kbar: Role of vacancies. American Mineralogist, 74, 1287-1292.

Mitreikina, O.B., Chryukina, O.V., Zinovieva, N.G., and Granovsky, L.B. (1994) Mineral paragenesis of the ureilites: Evidence for high pressure in a large parent body (abstract). Lunar and Planetary Science, XXV, 909-910.

Miyamoto, M., Fujii, N., and Takeda, H. (1981) Ordinary chondrite parent body: An internal heating model. Proc. Lunar and Planetary Science Conf. 12B, 1145-1152.

Naemura, K., Hirajima, T., and Svojtka, M. (2009) The pressure–temperature path and the origin of phlogopite in spinel–garnet peridotites from the Blansk Les massif of the Moldanubian zone, Czech Republic Journal of Petrology, 50, 1795-1827.

Nickel, K.G. and Green, D.H. (1985) Empirical geothermometry for garnet peridotites and implications for the nature of the lithosphere, kimberlites and diamonds. Earth and Planetary Science Letters, 73, 158-170.

Nimis, P. and Taylor, W.R. (2000) Single clinopyroxene thermometry for garnet peridotite. Part I. Calibration and testing of a Cr-in-Cpx barometer and an enstatite-in-Cpx thermometer. Contributions to Mineralogy and Petrology, 139, 541-554.

Ohtani E., Kimura Y., Kimura M., Takata T., Kondo T., and Kubo T. 2004. Formation of high-pressure minerals in shocked L6 chondrite Yamato 791384: constraints on shock conditions and parent body size. Earth and Planetary Science Letters 227: 505-515.

O'Neill, H.S.C. and Wood, B.J. (1979) An experimental study of Fe-Mg partitioning between garnet and olivine and its calibration as a geothermometer. Contributions to Mineralogy and Petrology, 70, 59-70.

Ota, K., Mikouchi, T., and Sugiyama, K. (2009) Crystallography of hornblende amphibole in LAP04840 R chondrite and implication for its metamorphic history. Journal of Mineralogical and Petrological Sciences, 104, 215-225.

Righter, K. and Drake, M.J. (1996) Core formation in Earth's Moon, Mars, and Vesta. Icarus, 124, 513-529.

Righter, K. and Neff, K.E. (2007) Temperature and oxygen fugacity constraints on CK and R chondrites and implications for water and oxidation in the early solar system. Polar Science, 1, 25-44.

Semenenko V. P., Girich A. L., and Nittler L. R. (2004) An exotic kind of cosmic material: graphite-containing xenoliths from the Krymka (LL3.1) chondrite. Geochimica et Cosmochimica Acta, 68, 455-475.

Sugiura, N., Takehana, Y., Hiyagon, H., and Kita, N.T. (2008) An igneous clast with both graphite-bearing and graphite-free lithologies in the Northwest Africa 801 CR2 chondrite (abstract). Meteoritics and Planetary Science, 43, A149.

Taylor, W.R. (1998) An experimental test of some geothermometer and geobarometer formulations for upper mantle peridotites with application to the thermobarometrty of fertile lherzolite and garnet websterite. Neues Jahrbuch für Mineralogie. Abhandlungen, 172, 381-408.

Weisberg, M.K. and Kimura, M. (2010) Petrology and Raman spectroscopy of high pressure phases in the Gujba CB chondrite and the shock history of the CB parent body. Meteoritics and Planetary Science, 45, 873-884.

Weisberg, M.K., Prinz, M., Clayton, R.N., and Mayeda, T.K. (1993) The CR (Renazzo-type) carbonaceous chondrite group and its implications. Geochimica et Cosmochimica Acta, 57, 1567-1586.

CAPTIONS FOR FIGURES

Figure 1. Back-scattered electron images of a clast in the NWA 801 (CR) chondrite. a) The whole area of clast #6 showing a sharp boundary against the matrix and chondrules. The clast consists of silicate minerals and abundant weathering products including opaque minerals (bright). The boundary between the clast and matrix and chondrules is shown by white arrows. Width of field is 1.8mm. b) A detailed image of clast #2 showing granular texture. The constituent minerals are olivine (Ol), orthopyroxene (Opx), garnet (Grt), and omphacite (Omp), with minor graphite (Gr) and apatite (Ap). The irregular-shaped bright area consists of Fe-Ni metal, sulfide, and their weathering products. Width of field is 280μm. c) A coarse orthopyroxene grain containing a Mg-rich core (dark areas in Opx, En_{79-84}) in clast #2. Width of field is 120μm.

Figure 2. An atomic Ca-Mg-Fe diagram for orthopyroxene in the clasts. Mg-rich pyroxene (up to $En_{87}Wo_3$) is encountered in the cores of coarse grains and most of them are nearly homogeneous in composition ranging from $En_{70-75}Wo_{0.3-1.1}$.

Figure 3. Omphacite compositions in the clasts plotted on the atomic (Di+Hd)-(En+Fs)-(Jd+Kos) diagram. The omphacites not only contain Na-pyroxene (mainly jadeite) and diopside-hedenbergite components, but a significant enstatite-ferrosilite component. Di: diopside, Hd: hedenbergite, En: enstatite, Fs: ferrosilite, Jd: jadeite, Kos: kosmochlor

Figure 4. The atomic Ca-Mg-Fe diagram for garnet in the clasts. The garnets are pyrope-rich and homogeneous in composition.

Figure 5. (a) EBSD pattern of omphacite in NWA 801 clast #6. (b) The matching calculated pattern is omphacite with a C2/c structure (after McCormick et al. 1989).

Figure 6. Pressure-temperature estimate for a mineral assemblage in clast #6 based on a set of

geothermobarometries using olivine, pyroxenes, and garnet. The diamond-graphite boundary is from Bundy (1980). The square (dashed gray lines) indicates the estimated temperature and pressure condition for the clasts in NWA 801.

Table 1. Mineral assemblages of clasts in NWA 801.

Clast	Olivine*	Orthopyroxene*	Omphacite	Garnet	Phlogopite	Apatite	Graphite	Fe-Ni metal	Troilite	Pentlandite
#2 Graphite-bearing	67.2	73.0 / 0.8	++	++		+	+	+	+	+
#2 Graphite-free	67.0		++	++	+	+		+	+	+
#3	67.2	73.5 / 0.7	++	++	+	+		+	+	+
#6	67.2	73.1 / 0.7	++	++	+	+	+	+	+	+

*: average Fo, **: average En/Wo, excluding Mg-rich core, ++: common, +: minor or rare

Table 2. Representative mineral compositions of clasts of NWA 801.

Clast	Note	SiO_2	TiO_2	Al_2O_3	Cr_2O_3	FeO	MnO	MgO	CaO	Na_2O	K_2O	P_2O_5	Cl	Total	O	Si	Ti	Al	Cr	Fe	Mn	Mg	Ca	Na	K	P	Cl	Total
#3	Apatite	0.24	b.d.	b.d.	b.d.	1.65	0.13	0.80	48.67	0.97	b.d.	41.81	4.40	98.67	12	0.021				0.117	0.009	0.102	4.434	0.162		3.009	0.633	8.487
#2	Garnet	40.25	0.08	20.95	2.16	20.52	0.90	12.30	3.03	0.07	b.d.	b.d.	b.d.	100.30	12	3.020	0.005	1.853	0.128	1.287	0.057	1.376	0.243	0.011				7.980
#6	Garnet	40.14	0.05	21.09	2.02	20.68	0.99	11.20	4.46	0.06	b.d.	b.d.	b.d.	100.70	12	3.016	0.002	1.868	0.120	1.300	0.064	1.254	0.358	0.008				7.992
#2	Olivine	37.35	b.d.	b.d.	b.d.	29.31	0.35	33.34	b.d.	b.d.	b.d.	b.d.	b.d.	100.44	4	1.000				0.656	0.008	1.331						2.997
#3	Olivine	36.95	b.d.	b.d.	b.d.	28.90	0.36	33.14	b.d.	b.d.	b.d.	b.d.	b.d.	99.44	4	0.999				0.654	0.008	1.336						2.999
#6	Olivine	37.26	b.d.	b.d.	b.d.	28.89	0.43	33.60	b.d.	b.d.	b.d.	b.d.	b.d.	100.19	4	0.999				0.648	0.010	1.343						3.000
#2	Omphacite	55.56	0.55	6.95	3.42	5.79	b.d.	10.47	11.64	5.77	b.d.	b.d.	b.d.	100.21	6	1.998	0.015	0.295	0.097	0.174		0.561	0.449	0.402				3.993
#3	Omphacite	55.16	0.25	7.60	3.66	7.28	0.13	11.28	8.48	5.92	b.d.	b.d.	b.d.	99.76	6	1.988	0.007	0.323	0.104	0.219	0.004	0.606	0.327	0.413				3.998
#6	Omphacite	54.87	0.67	9.40	2.10	6.99	0.13	10.53	10.02	5.83	b.d.	b.d.	b.d.	100.54	6	1.958	0.018	0.395	0.059	0.209	0.004	0.560	0.383	0.403				3.994
#2	Orthopyroxe	55.53	b.d.	0.25	0.43	14.64	0.19	28.38	0.17	0.16	b.d.	b.d.	b.d.	99.77	6	1.994		0.010	0.012	0.440	0.006	1.519	0.006	0.011				3.999
#2	Orthopyroxe	56.62	0.00	0.24	0.49	10.56	0.20	31.02	0.16	0.12	b.d.	b.d.	b.d.	99.41	6	2.000		0.010	0.014	0.312	0.006	1.633	0.006	0.008				3.989
#3	Orthopyroxe	55.49	b.d.	0.94	0.43	16.55	0.28	26.28	0.31	0.43	b.d.	b.d.	b.d.	100.71	6	1.991		0.040	0.012	0.497	0.008	1.406	0.012	0.030				3.997
#6	Orthopyroxe	55.64	b.d.	0.30	0.26	15.89	0.20	27.39	0.17	0.13	b.d.	b.d.	b.d.	99.98	6	2.002		0.013	0.007	0.478	0.006	1.469	0.006	0.009				3.990
#2	Phlogopite	39.83	3.50	13.77	1.19	10.96	0.29	17.48	0.14	0.93	8.31	b.d.	0.77	96.40	11	2.884	0.191	1.175	0.068	0.664	0.018	1.887	0.011	0.130	0.768		0.095	7.891

b.d.: below detection limits (3 σ , in wt.%), 0.04 for Al_2O_3, CaO, Na_2O, K_2O and Cl, 0.05 for TiO_2, 0.09 for P_2O_5, and 0.10 for Cr_2O_3 and MnO.

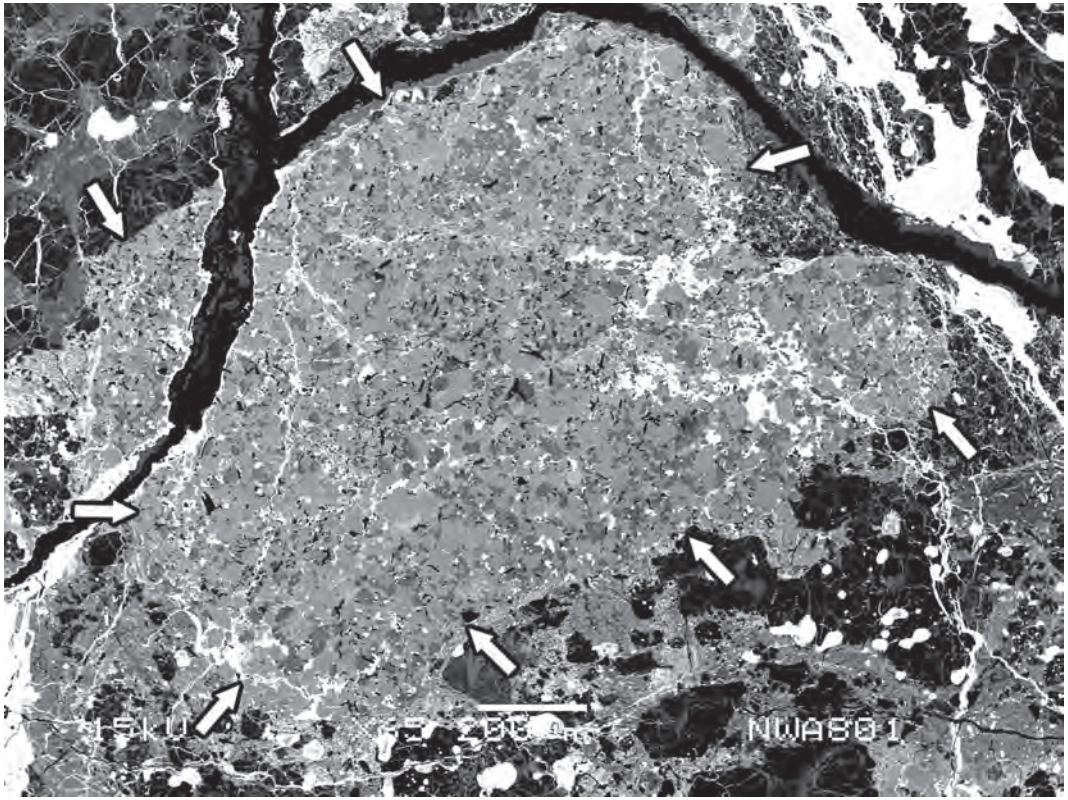

Fig. 1a

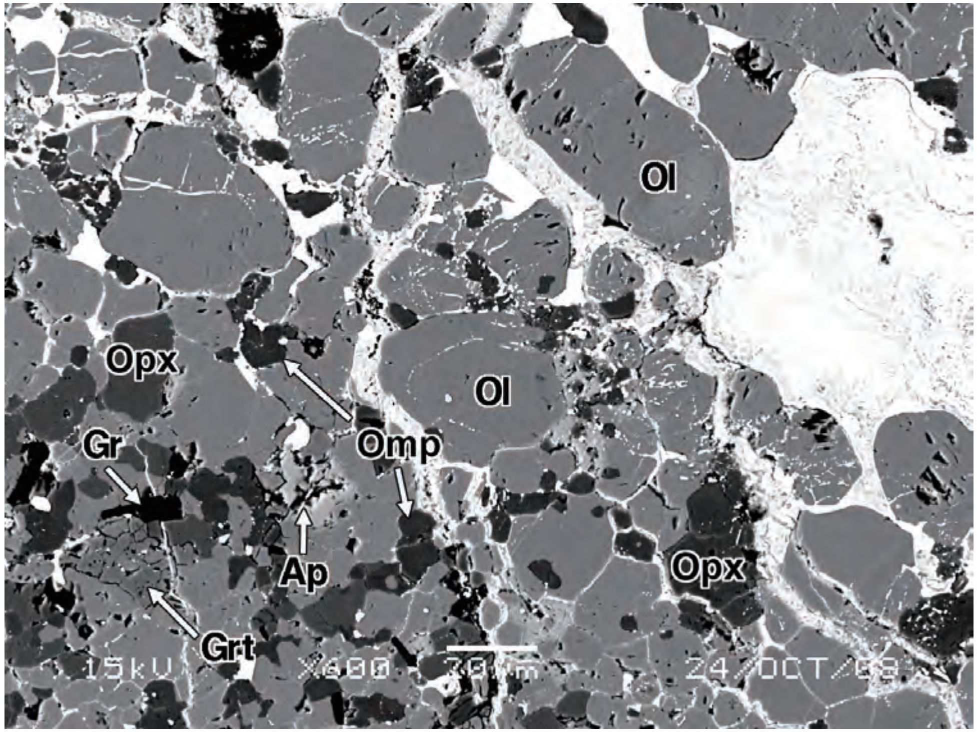

Fig. 1b

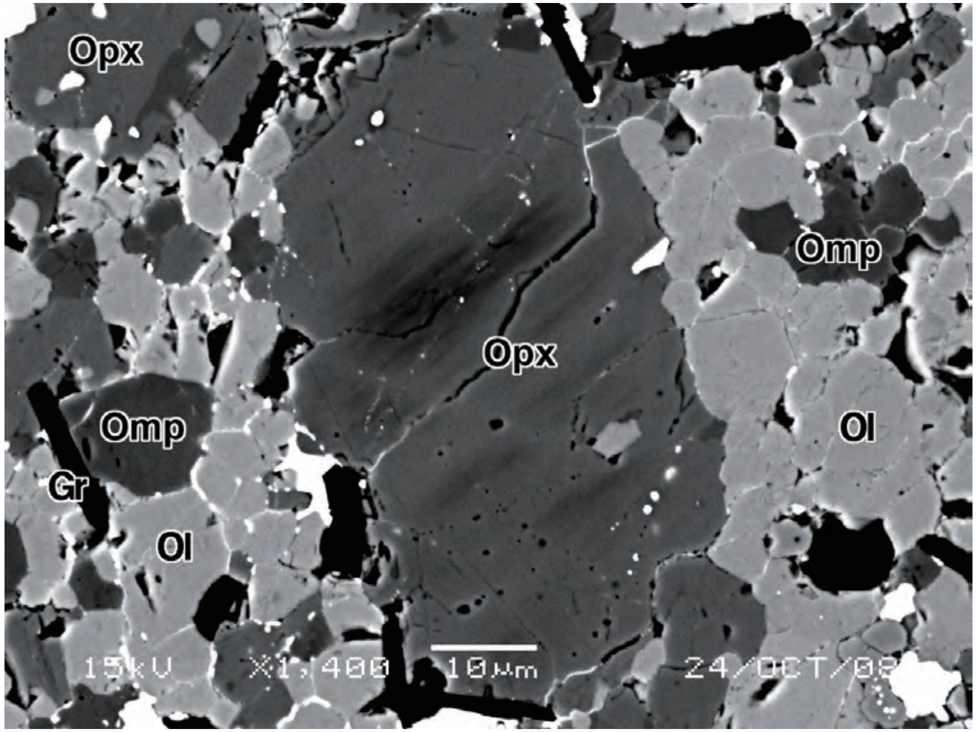

Fig. 1c

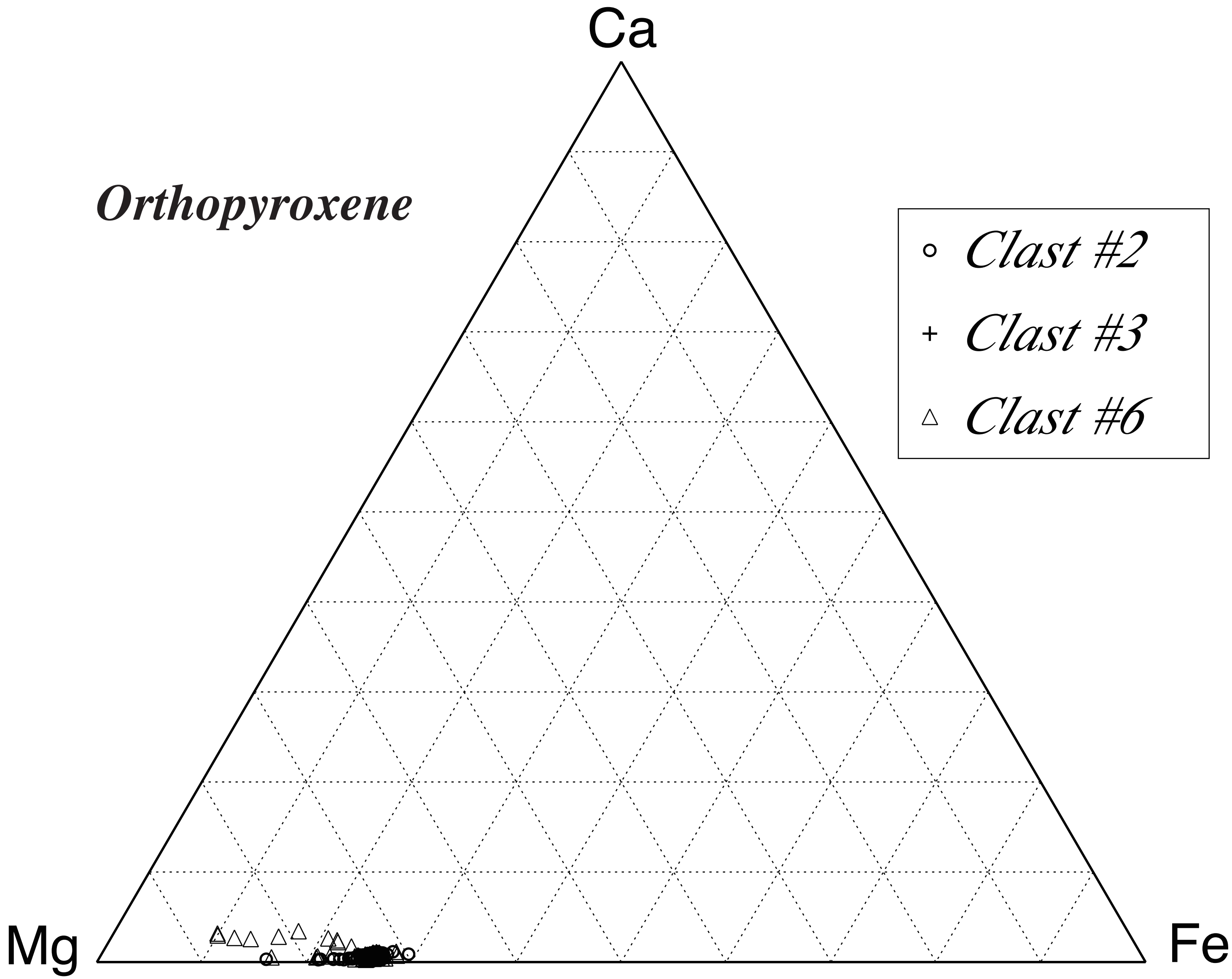

Fig. 2

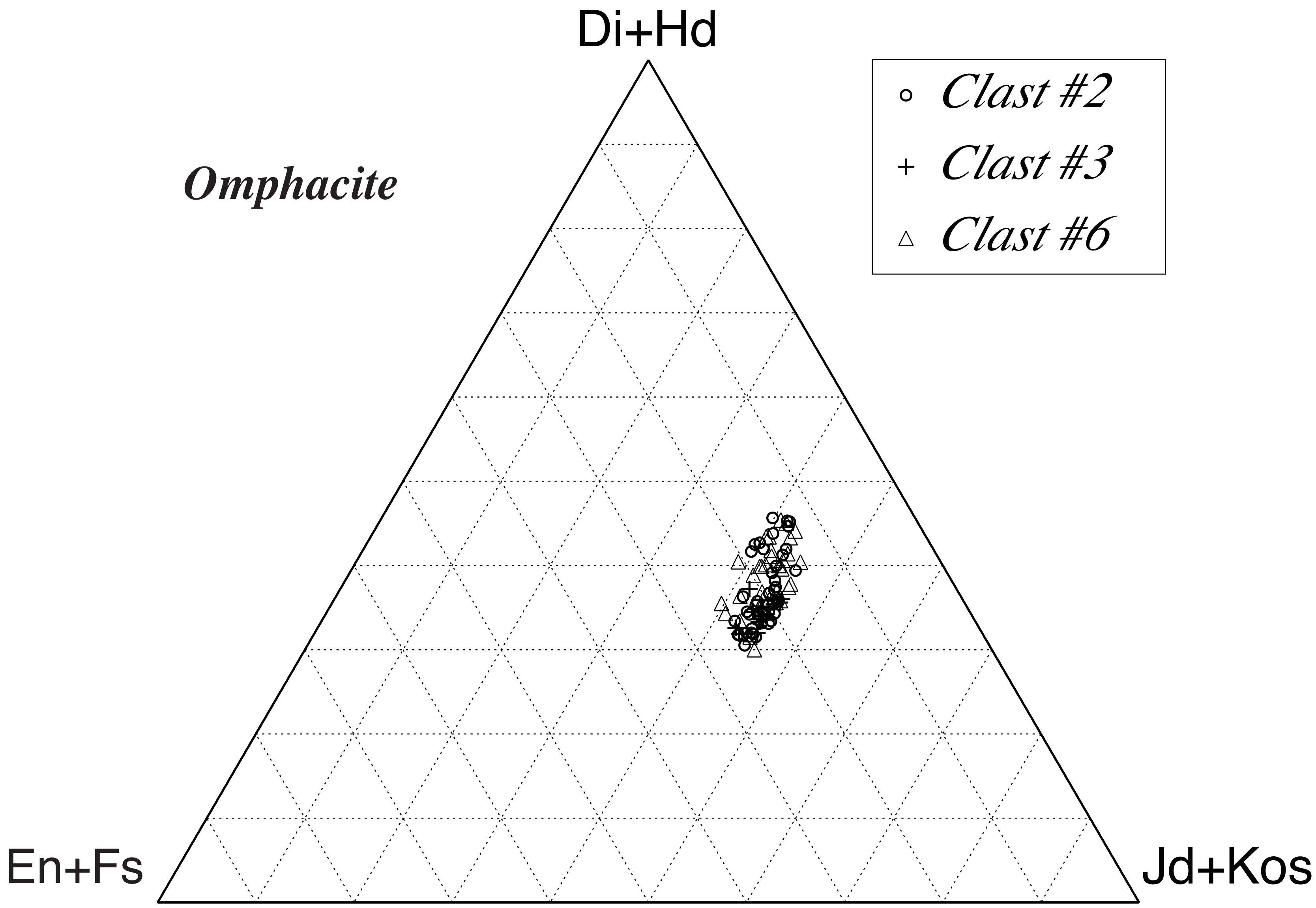

Fig. 3

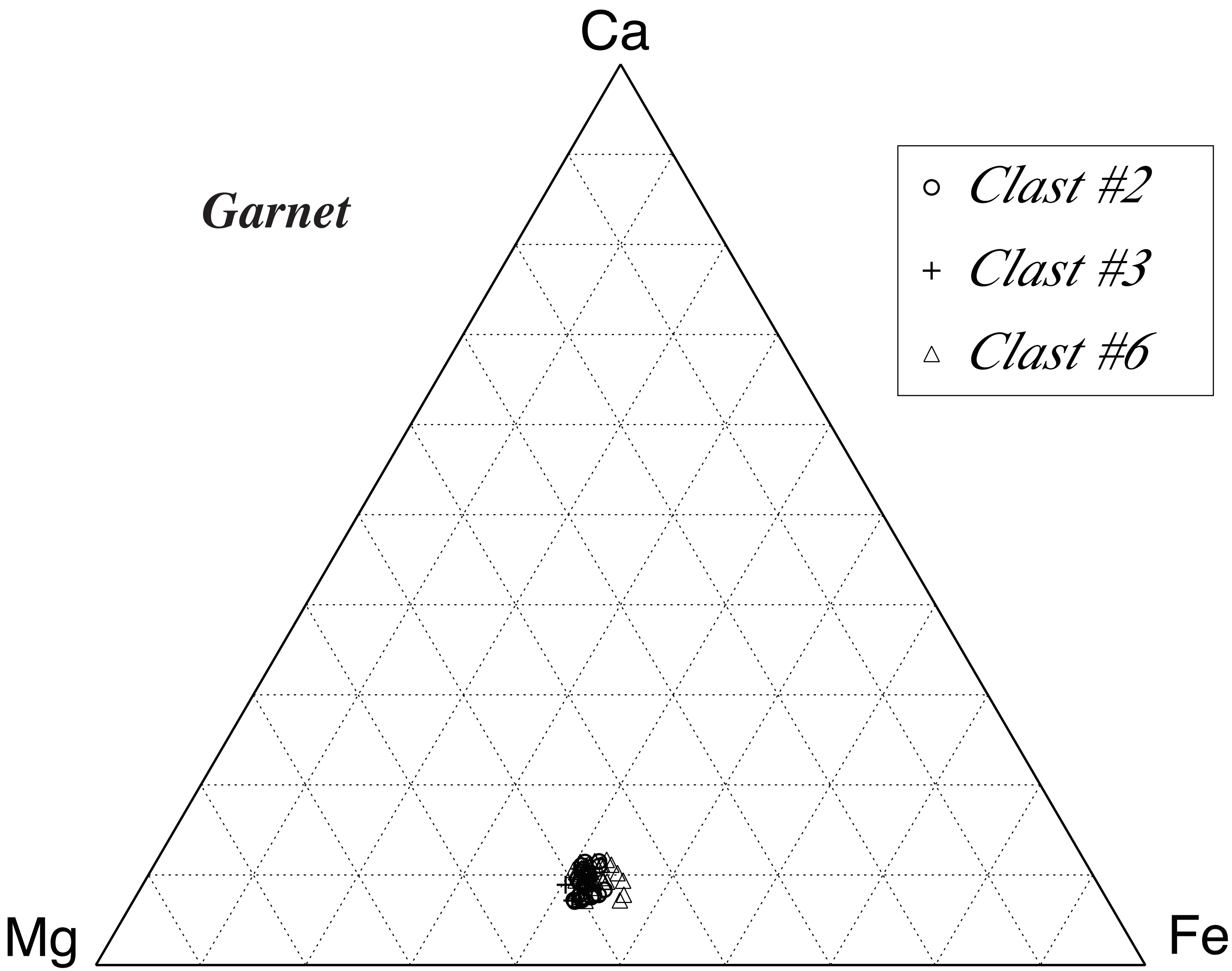

Fig. 4

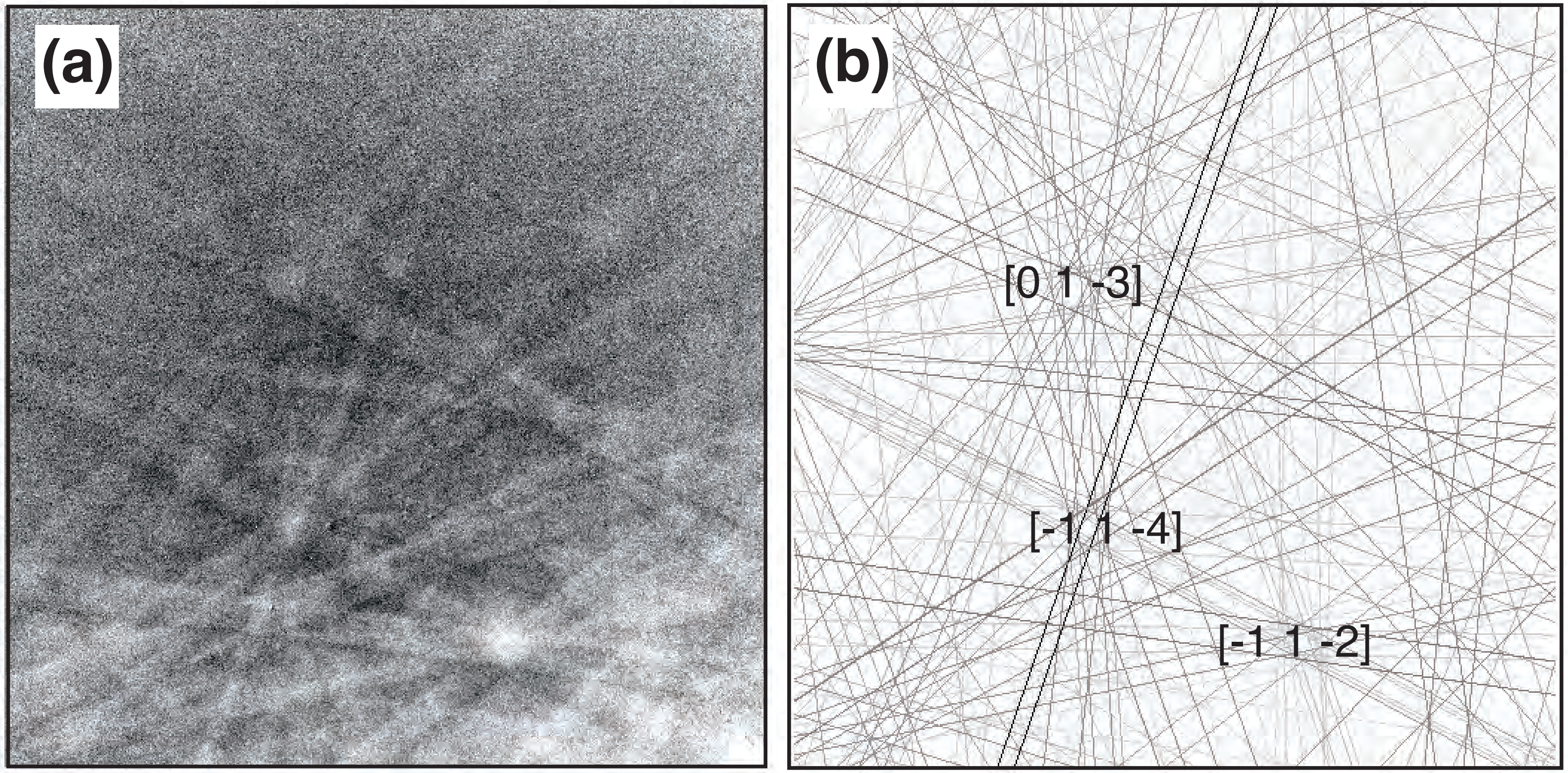

Fig. 5

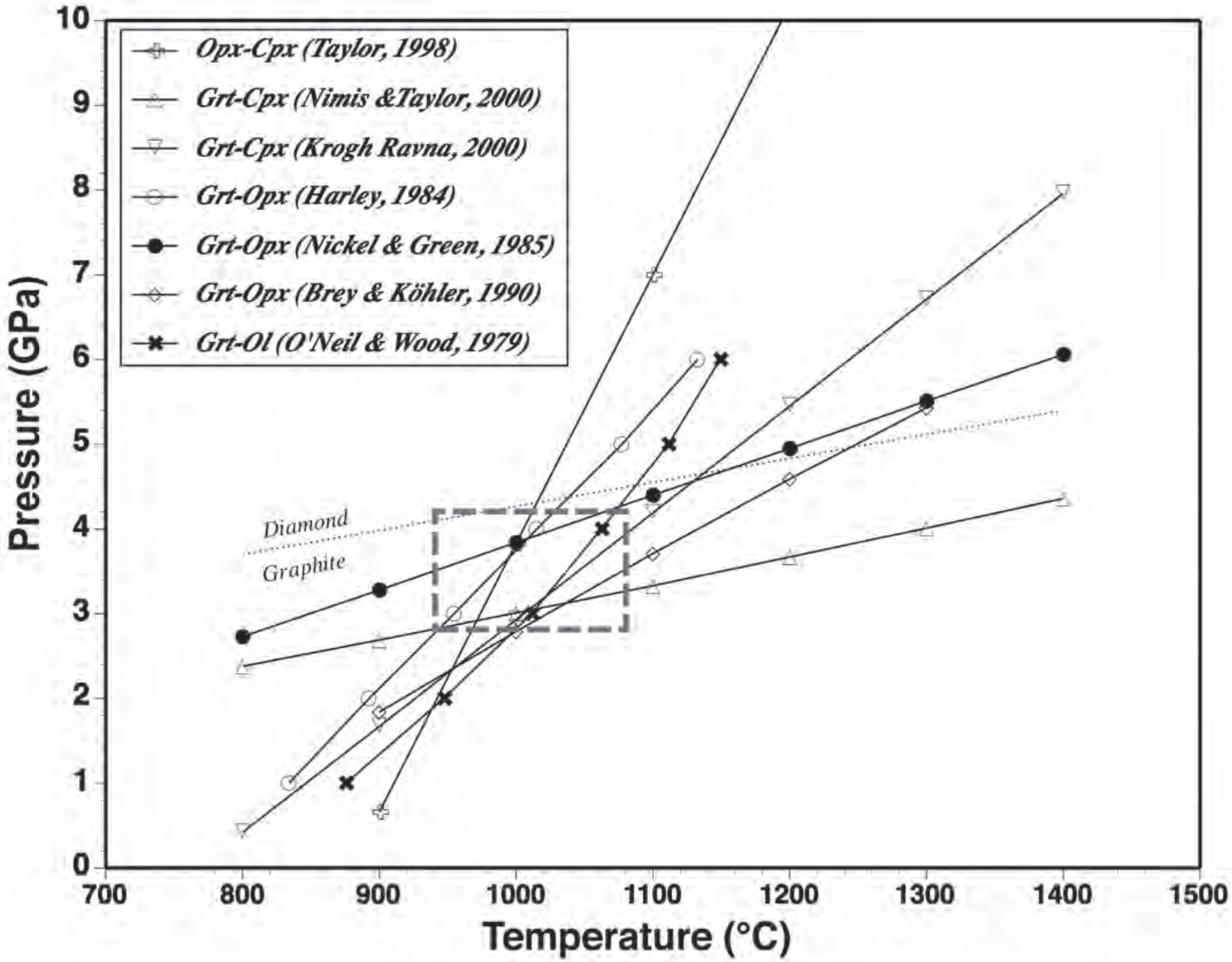

Opx-Cpx (Taylor, 1998)
Grt-Cpx (Nimis &Taylor, 2000)
Grt-Cpx (Krogh Ravna, 2000)
Grt-Opx (Harley, 1984)
Grt-Opx (Nickel & Green, 1985)
Grt-Opx (Brey & Köhler, 1990)
Grt-Ol (O'Neil & Wood, 1979)
Diamond
Graphite
Pressure (GPa)
Temperature (°C)
0
1
2
3
4
5
6
7
8
9
10
700
800
900
1000
1100
1200
1300
1400
1500

Fig. 6